

Supporting Information

Modulating Charge Migration in Photoredox Organic Transformation via Exquisite Interface Engineering

Shuai Xu, Ming-Hui Huang, Tao Li, Zhi-Quan Wei, Xin Lin, Xiao-Cheng Dai, Shuo Hou, Xiao-Yan Fu, Fang-Xing Xiao*

College of Materials Science and Engineering, Fuzhou University, New Campus, Minhou, Fujian
Province 350108, China.

Email: fxxiao@fzu.edu.cn

Table of Contents

	Page NO.
Fig. S1. Sample color of blank SnO ₂ NSs, SP-10, SC, and SPC-10 heterostructures	S3
Fig. S2. UV-vis absorption spectra of PDDA aqueous solution	S4
Fig. S3. Size distribution histogram of SnO ₂ NSs	S5
Fig. S4. TEM and FESEM images along with corresponding EDS and elemental mapping results of samples	S6
Fig. S5. Photoactivities of SPC-10 toward photooxidation without adding catalyst or light irradiation	S7
Fig. S6. Control experiments of for different samples toward selective oxidation	S8
Fig. S7. XRD patterns of SrTiO ₃ , SrC, SrPC-10, TiO ₂ , TC, and TPC-10 nanocomposite	S9
Fig. S8. UV-vis diffuse reflectance spectra (DRS) for different samples	S10
Fig. S9. SEM, EDS, and elemental mapping images of SrPC-10 and TPC-10 heterostructures	S11
Fig. S10. GC spectrum illustrating the detailed selective oxidation for different samples	S12
Fig. S11. GC spectrum illustrating the detailed selective oxidation for different samples	S12
Fig. S12. GC spectrum illustrating the detailed selective oxidation for different samples	S12
Fig. S13. 4-NA photoreduction without adding catalyst or light irradiation	S13
Fig. S14. UV-vis absorption spectra of 4-NA over SPC-10 heterostructures	S14
Fig. S15. Control experiments of different samples toward 4-NA photoreduction	S15
Fig. S16. XRD patterns of SPC-10 heterostructure before and after cyclic photoreduction reactions	S16
Fig. S17. Survey and high-resolution of SPC-10 heterostructure before and after reactions	S17
Fig. S18. CV of (a) BA and (b) BAD, (c) Mott-Schottky and (d) Band positions of CdS	S18
Fig. S19. Schematic illustration of photocatalytic mechanism of SPC nanocomposites	S19
Table S1. Functional groups vs. wavenumber for different samples	S20
Table. S2. Specific surface area, pore volume and pore size for three samples	S20
Table. S3. Chemical bond species vs. B.E. for different samples	S21

Table S4. Photoactivities of different samples toward selective oxidation.....	S22
Table S5. Photooxidation performances of a series of aromatic alcohols.....	S23
Table S6. Photoactivities of different samples toward 4-NA photoreduction	S24
Table S7. Photoreduction performances of a series of nitroaromatic compounds.....	S25
Experimental section: Preparation of different samples.....	S26

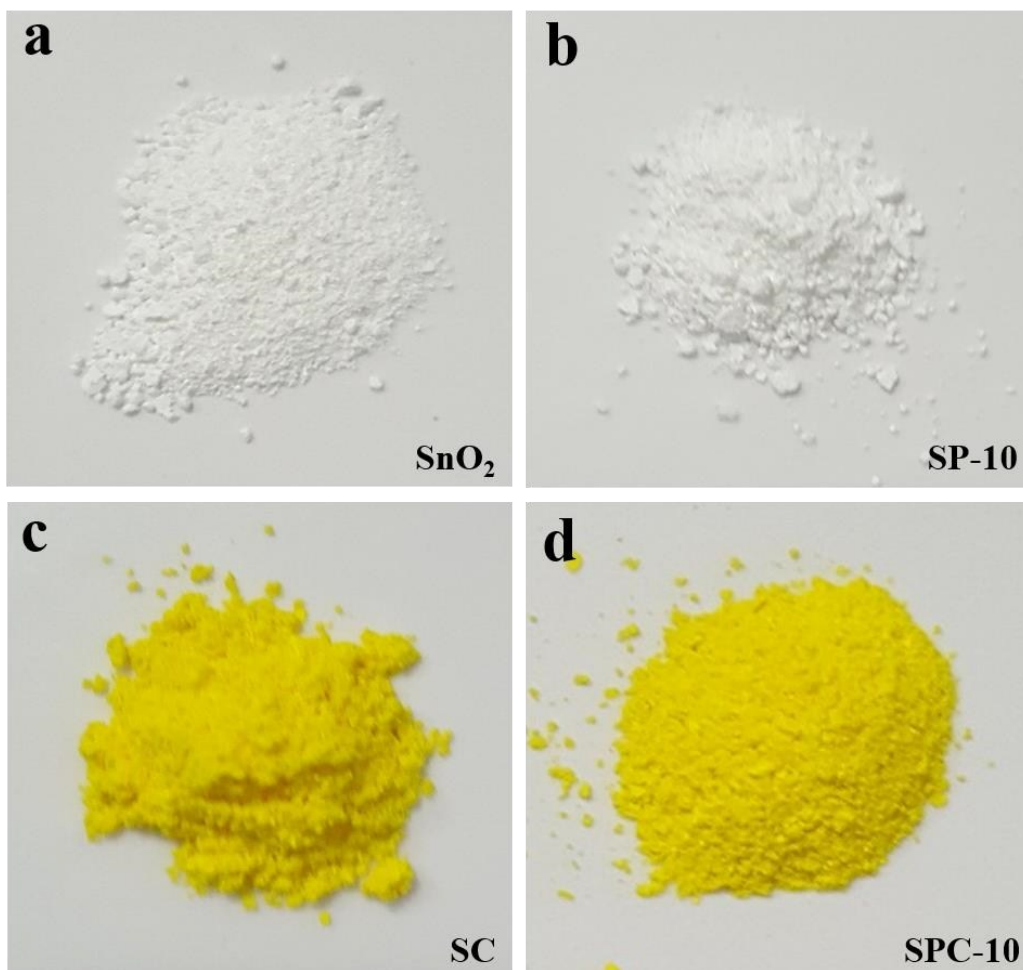


Fig. S1. Sample color of (a) SnO_2 NSs, (b) SP-10, (c) SC and (d) SPC-10.

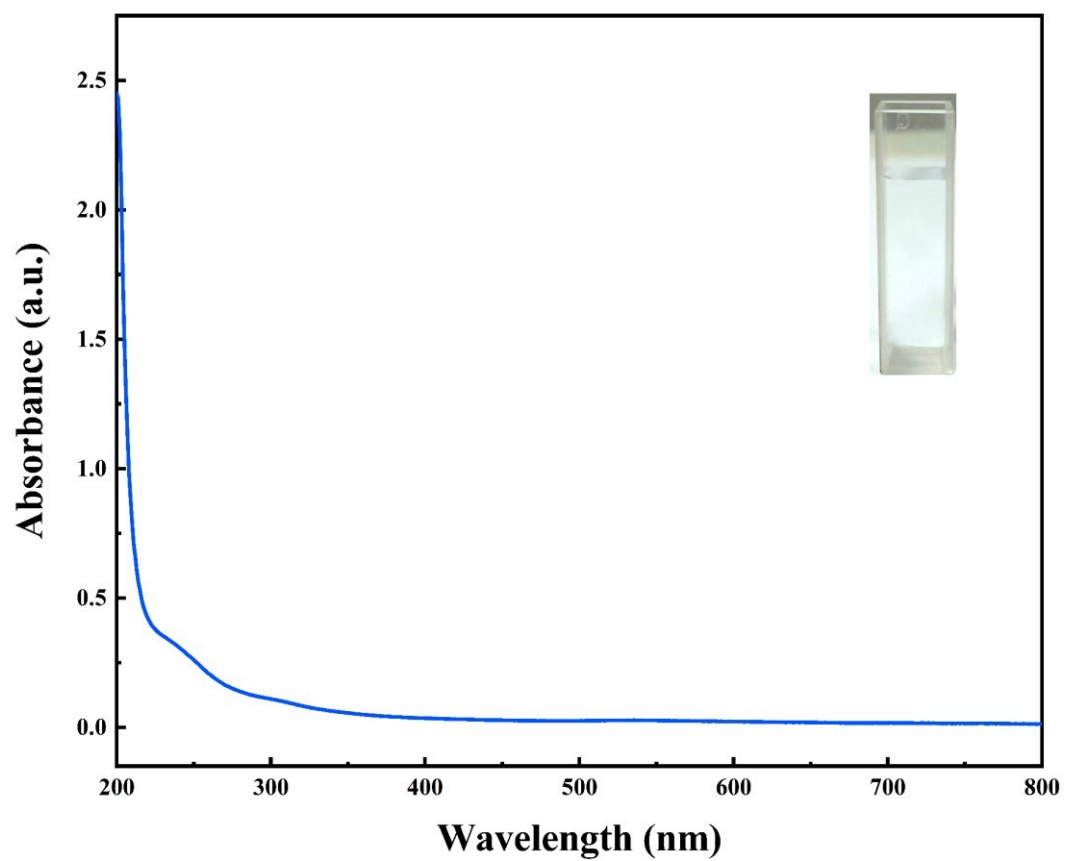


Fig. S2. UV-vis absorption spectrum of PDDA aqueous solution.

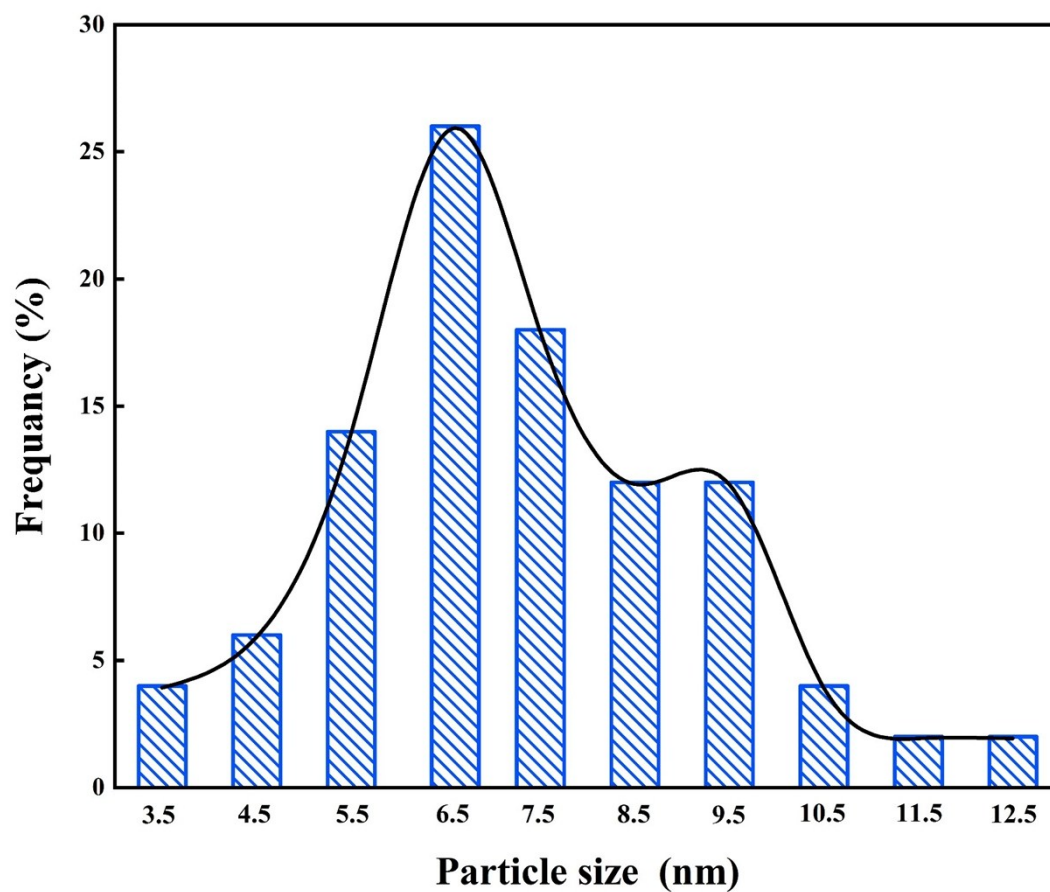


Fig. S3. Size distribution histogram of SnO₂ NSs obtained from TEM image.

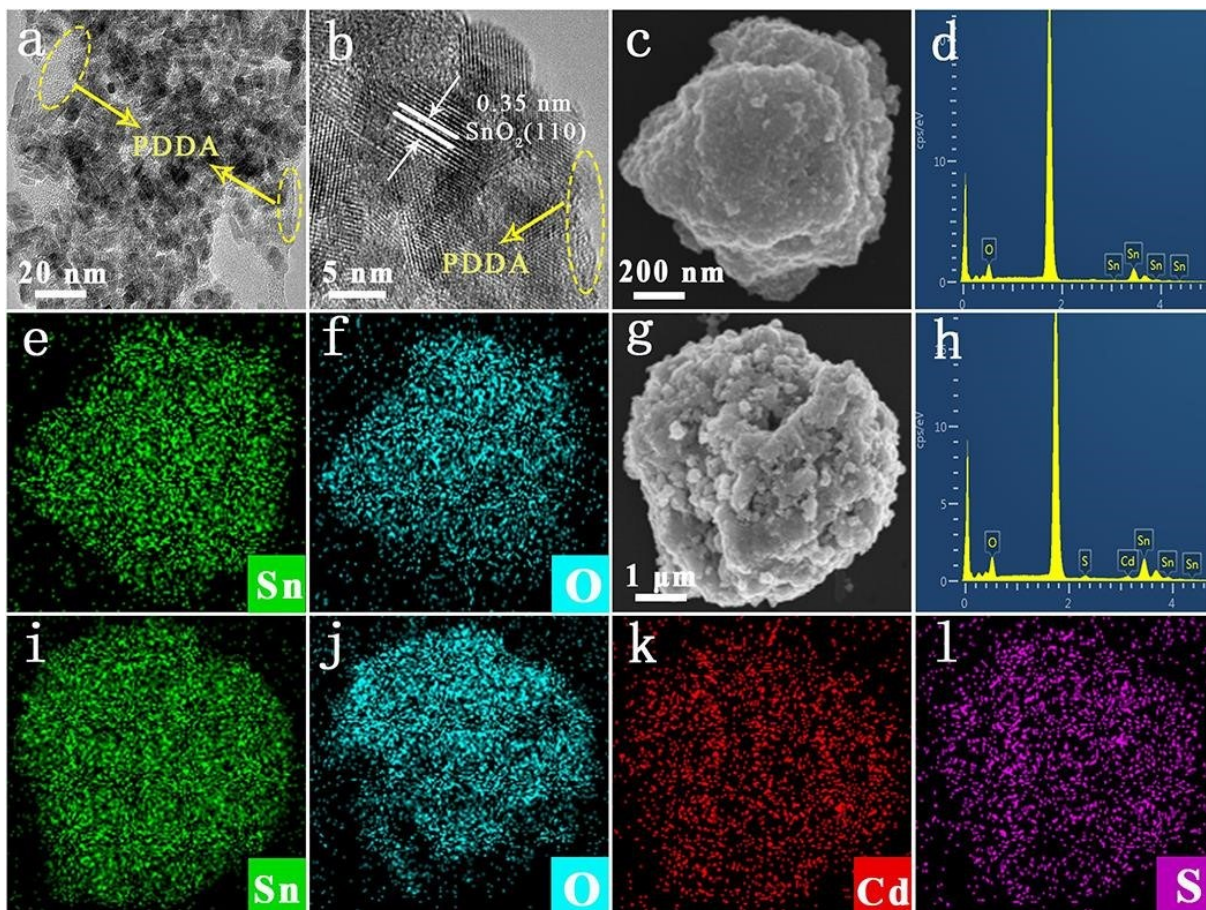


Fig. S4. TEM & HRTEM images of (a-b) SP-10 and FESEM images along with EDS and elemental mapping results of (c-f) SnO₂ NSs and (g-l) SC.

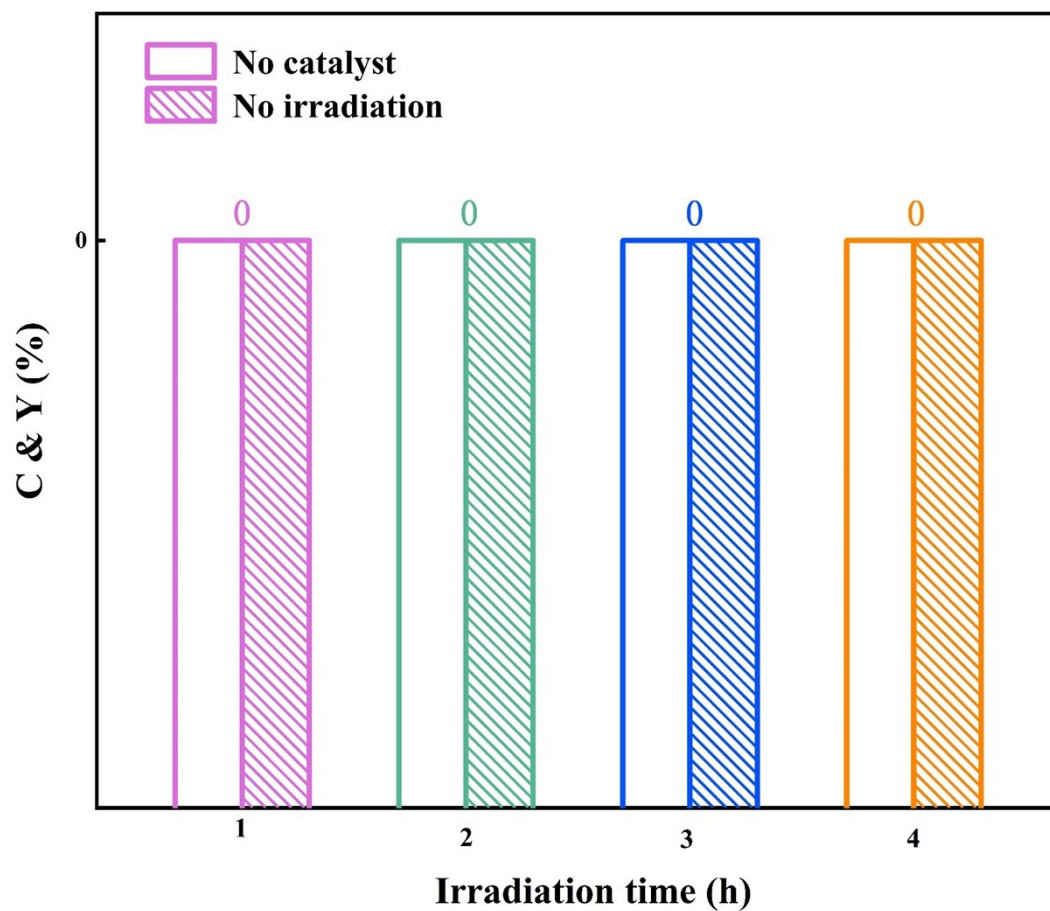


Fig. S5. Photoactivities of SPC-10 toward oxidation of BA to BAD without adding catalyst or light irradiation.

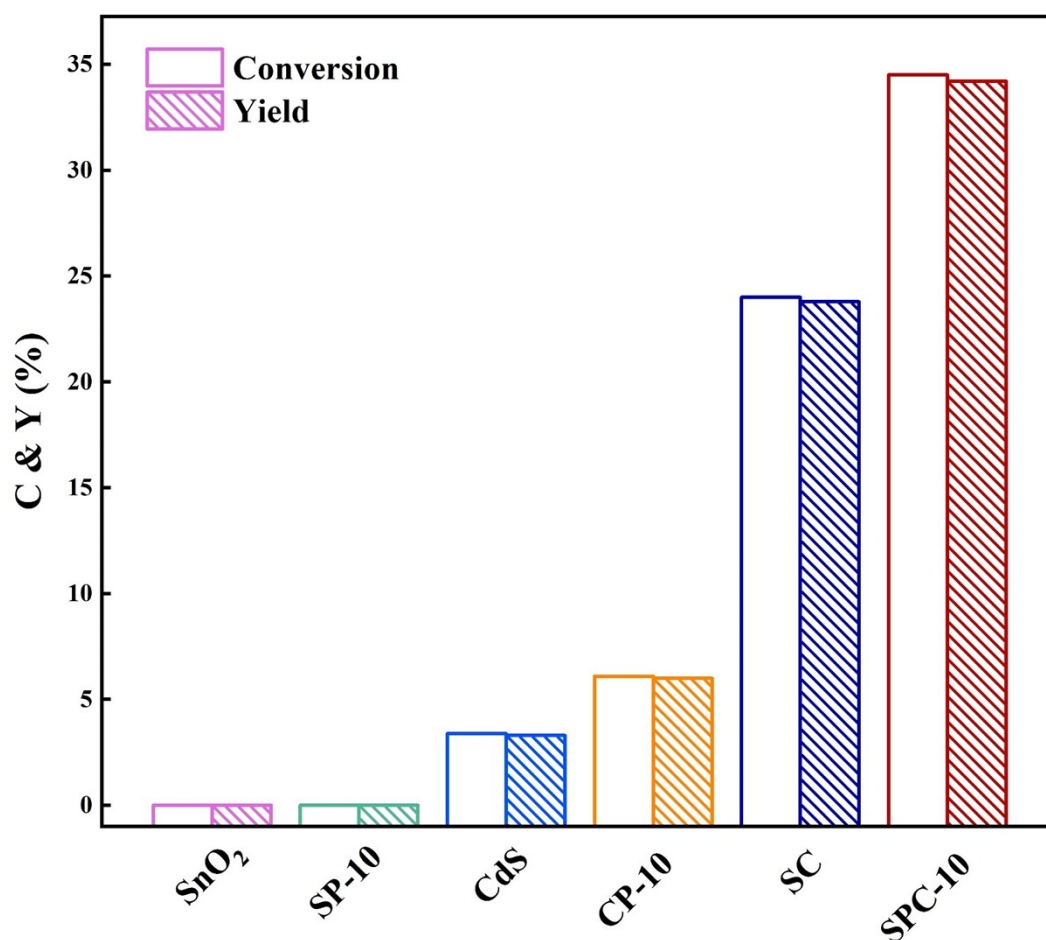


Fig. S6. Photoactivities of SnO₂ NSs, SP-10, CdS, CP-10, SC, and SPC-10 toward selective oxidation of BA to BAD under visible light irradiation ($\lambda > 420$ nm) for 4 h.

Note: Fig. S6 shows SPC-10 always exhibit the optimal photoactivity compared with other counterparts under the same conditions. Specifically, SC demonstrate remarkably enhanced photoactivity relative to CdS, which is caused by the cooperativity of CdS and SnO₂ NSs in terms of their favorable energy level alignment. Notably, both CP-10 and SPC-10 exhibit considerably enhanced photoactivities compared with CdS and SC, confirming the pivotal role of PDDA in improving the interfacial electron transfer. It is worth noting that photoactivities of SP-10 and SnO₂ NSs are the same and tend to be zero, which is due to the large bandgap of SnO₂ NSs that is difficult to be photoexcited under visible light irradiation, failing to produce electron-hole pairs. As such, even if ultra-thin PDDA layer was wrapped on the SnO₂ NSs surface, photoactivity of SP-10 was not improved.

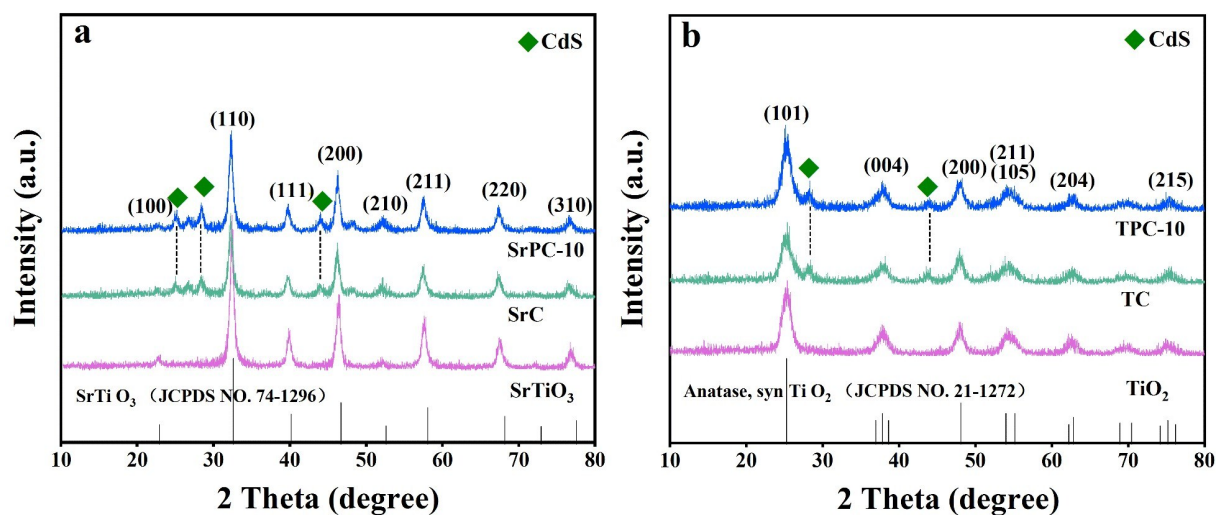


Fig. S7. XRD patterns of (a) SrTiO₃, SrC, SrPC-10 and (b) TiO₂, TC, TPC-10.

Note: As shown in **Fig. S7a**, XRD patterns of SrTiO₃, SrC, and SrPC-10 are similar, for all of which the peaks at 22.75, 32.40, 39.96, 46.47, 57.79, and 67.82° are indexed to the cubic perovskite SrTiO₃ (JCPDS No. 74-1296). Analogous XRD patterns of SrC and SrPC-10 indicate compact CdS and PDDA encapsulation do not change the lattice structure of SrTiO₃. As well, as shown in **Fig. S7b**, XRD patterns of TiO₂, TC, and TPC-10 are similar, for all of which the peaks at 25.28, 36.94, 48.05, and 75.03 are indexed to anatase TiO₂ (JCPDS No. 21-1272). Notably, obvious peaks assignable to CdS can be distinguished in the XRD patterns of SrC, SrPC-10, TC, and TPC-10, for all of which the peaks at 24.8, 26.6, 28.2, 36.6, 43.7, 47.9, 50.9, 51.8, 52.8, 66.8, 69.2, 70.9, 72.3 and 75.4° are indexed to the hexagonal phase CdS (JCPDS No. 41-1049).

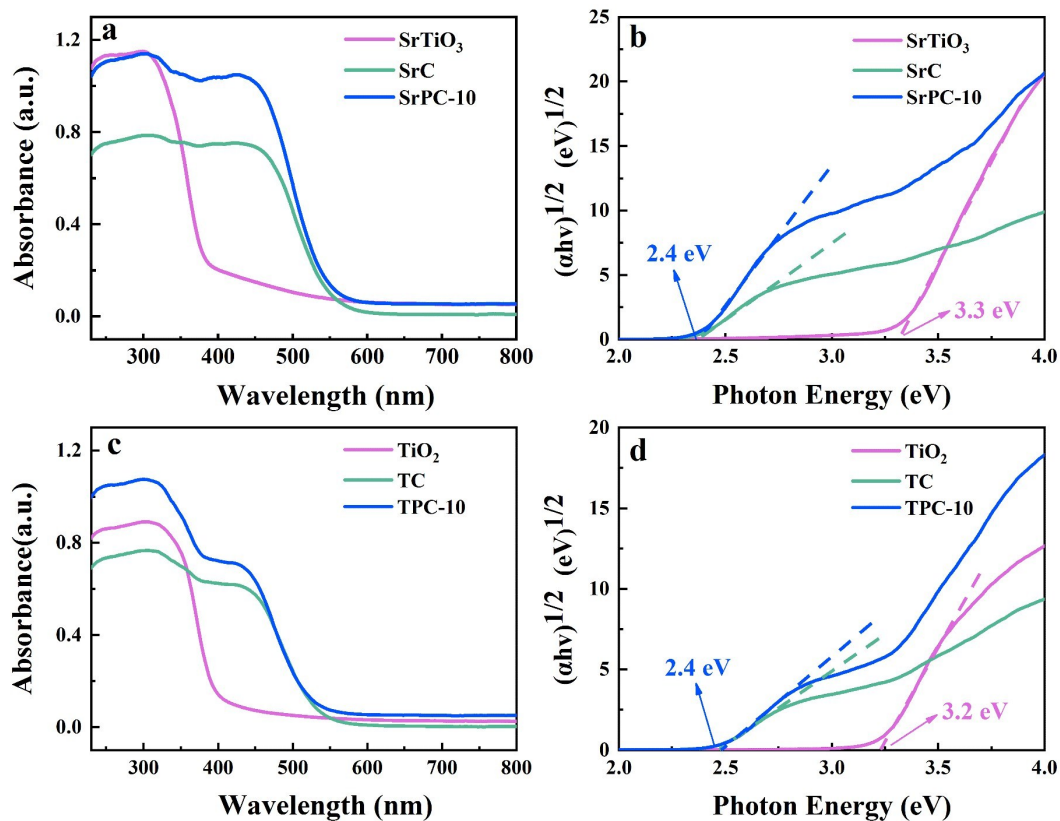


Fig. S8. DRS results with transformed plots based on the Kubelka-Munk function vs. photon energy for (a & b) SrTiO₃, SrC, SrPC-10 and (c & d) TiO₂, TC, TPC-10.

Note: As displayed in **Fig. S8(a & c)**, a broad absorption peak below 520 nm was observed in the DRS results of SrC, SrPC-10, TC, and TPC-10 and this is caused by the intrinsic band-gap-photoexcitation of CdS ingredient. Apparently, blank SrTiO₃ and TiO₂ do not demonstrate light absorption in the visible region owing to their wide bandgaps. Notably, light absorption band edges of SrPC-10 and TPC-10 were not changed in comparison with SC and TC, indicating ultra-thin PDDA encapsulation at the interface exerts no influence on the light absorption of SrPC-10 and TPC-10, which agrees well with the light absorption of PDDA aqueous solution (**Fig. S2**), eliminating the photosensitization effect of PDDA. According to the transformed plots based on Kubelka-Munk function vs. the energy of light, E_g values of binary and ternary nanocomposites were roughly determined, as displayed in **Fig. S8(b & d)**.

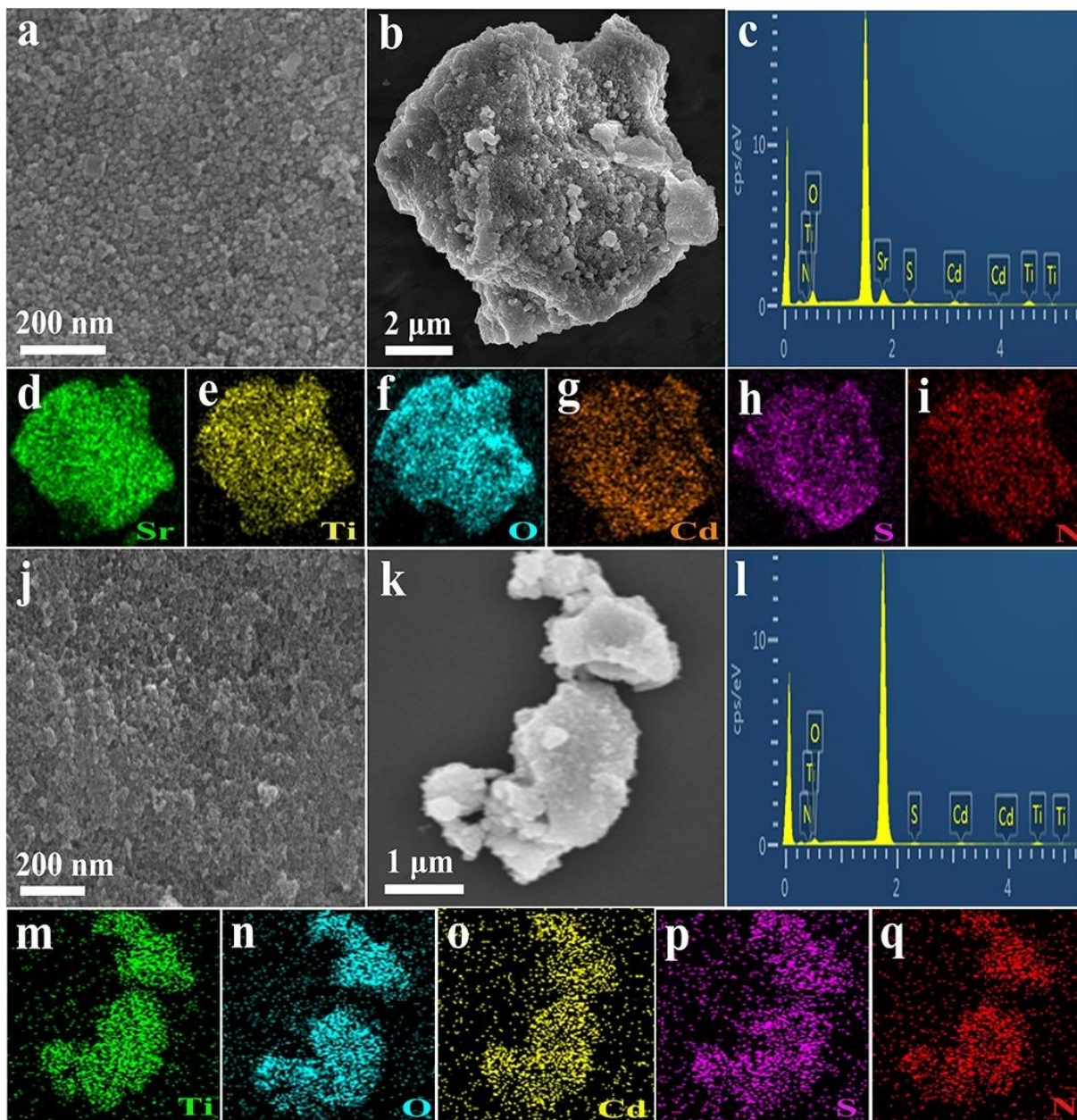


Fig. S9. FESEM images of (a) SrPC-10 & (j) TPC-10, and EDS results of (c) SrPC-10 & (l) TPC-10, with corresponding elemental mapping results of (d-i) SrPC-10 & (m-q) TPC-10.

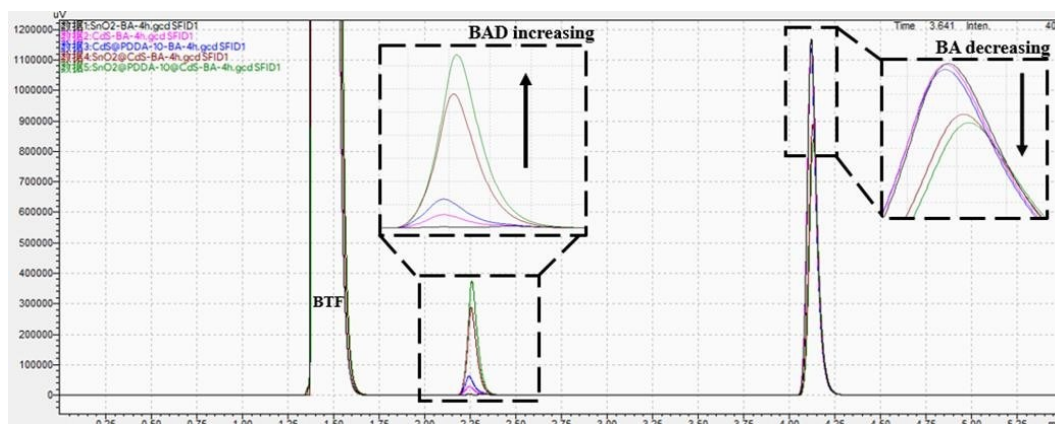


Fig. 10. GC spectrum illustrating selective oxidation of BA to BAD over SnO₂ NSs, CdS, CP-10, SC and SPC-10 under visible light irradiation ($\lambda > 420$ nm). The peaks from left to right correspond to BTF, BAD, and BA, respectively.

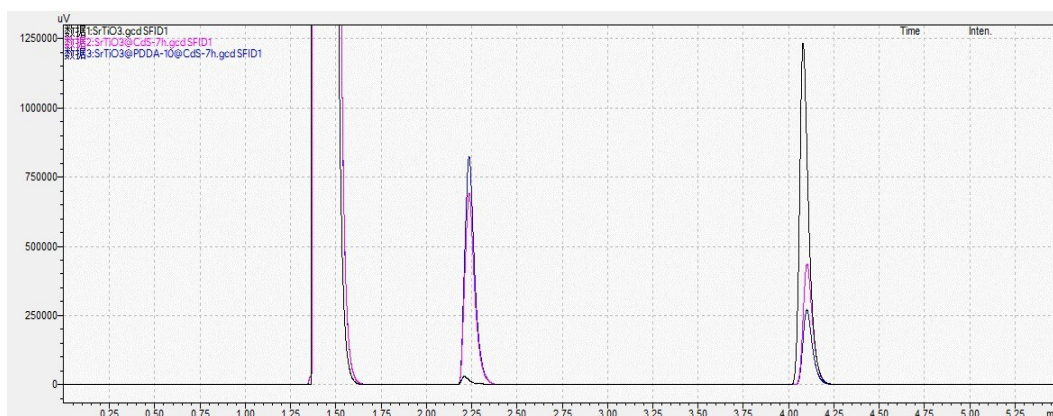


Fig. S11. GC spectrum illustrating selective oxidation of BA to BAD over SrTiO₃, SrC, and SrPC-10 under visible light irradiation ($\lambda > 420$ nm). The peaks from left to right correspond to BTF, BAD, and BA, respectively.

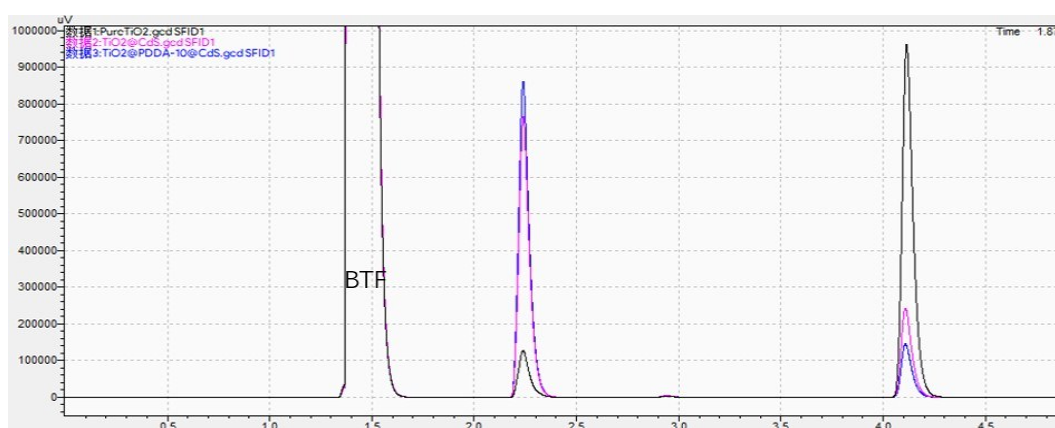


Fig. S12. GC spectrum illustrating selective oxidation of BA to BAD over TiO₂, TC, and TPC-10 under visible light irradiation ($\lambda > 420$ nm). The peaks from left to right correspond to BTF, BAD, and BA, respectively.

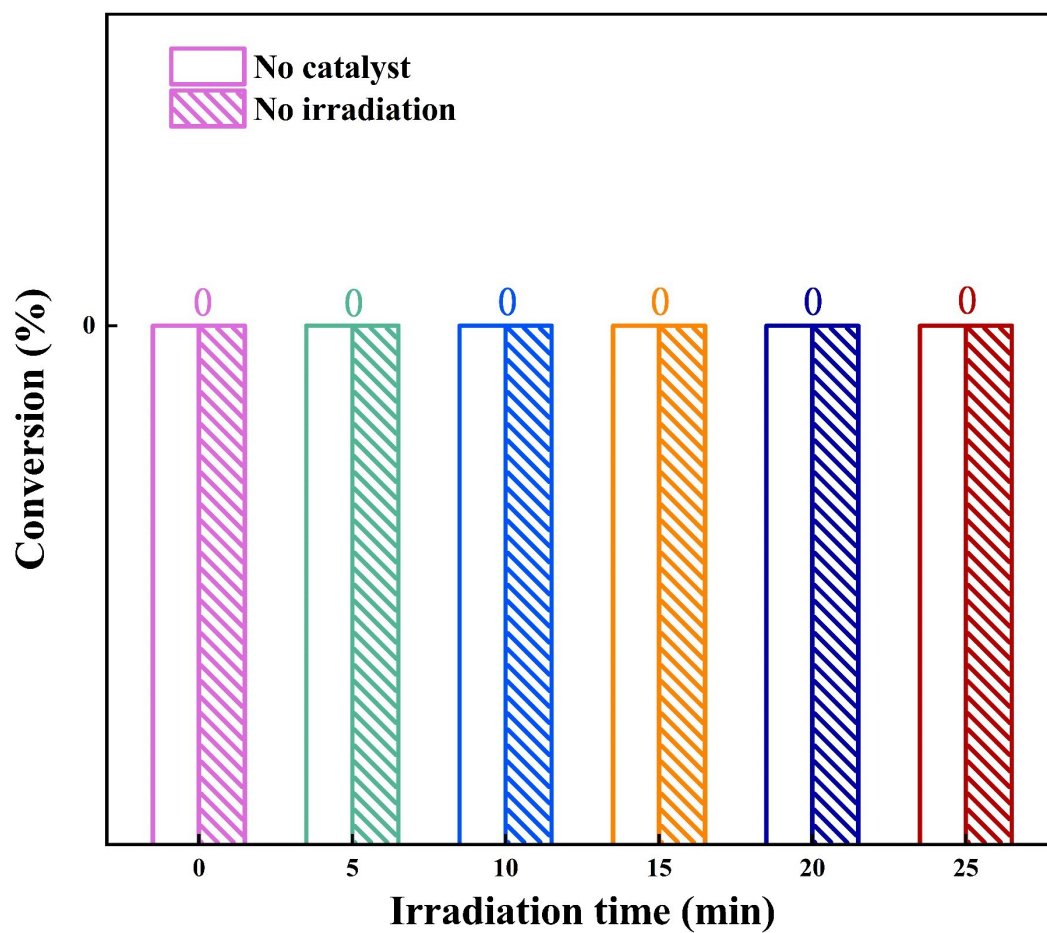


Fig. S13. Photoactivities of SPC-10 toward 4-NA photoreduction without adding catalyst or light irradiation.

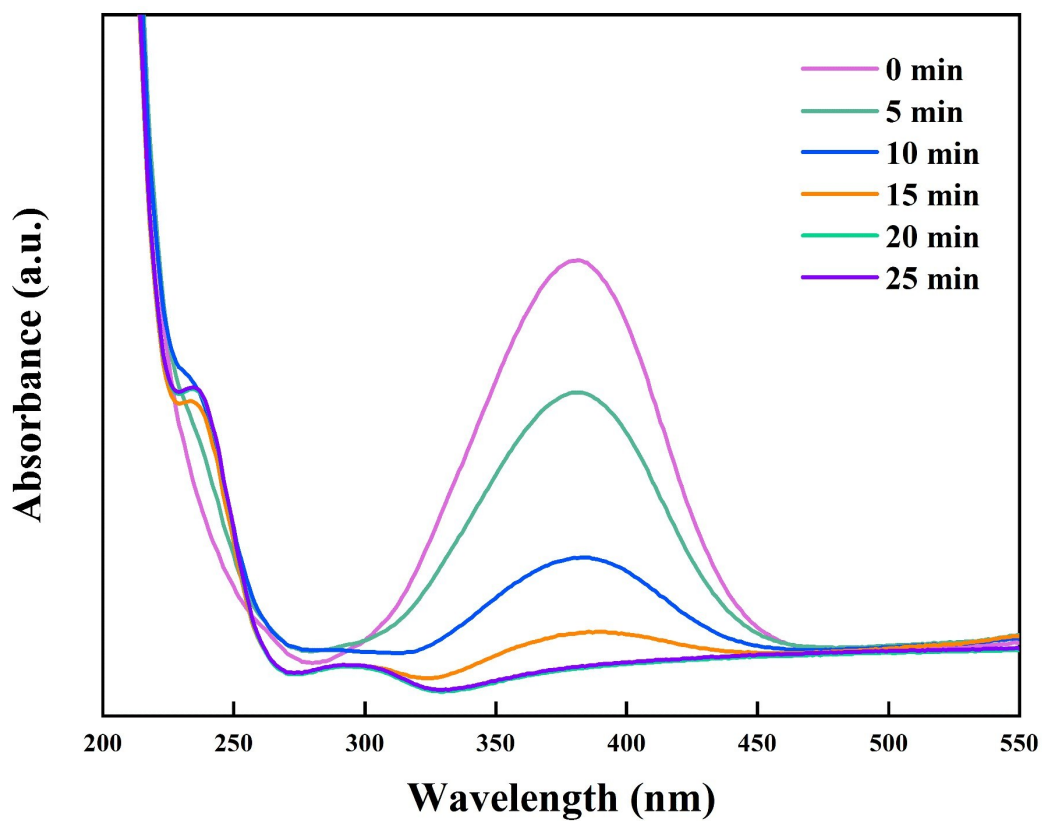


Fig. S14. UV-vis absorption spectra of 4-NA collected after designated irradiation time (25 min) when it was reduced over SPC-10 under visible light irradiation ($\lambda > 420$ nm) with the addition of ammonium formate as hole quencher and N_2 purge under ambient conditions.

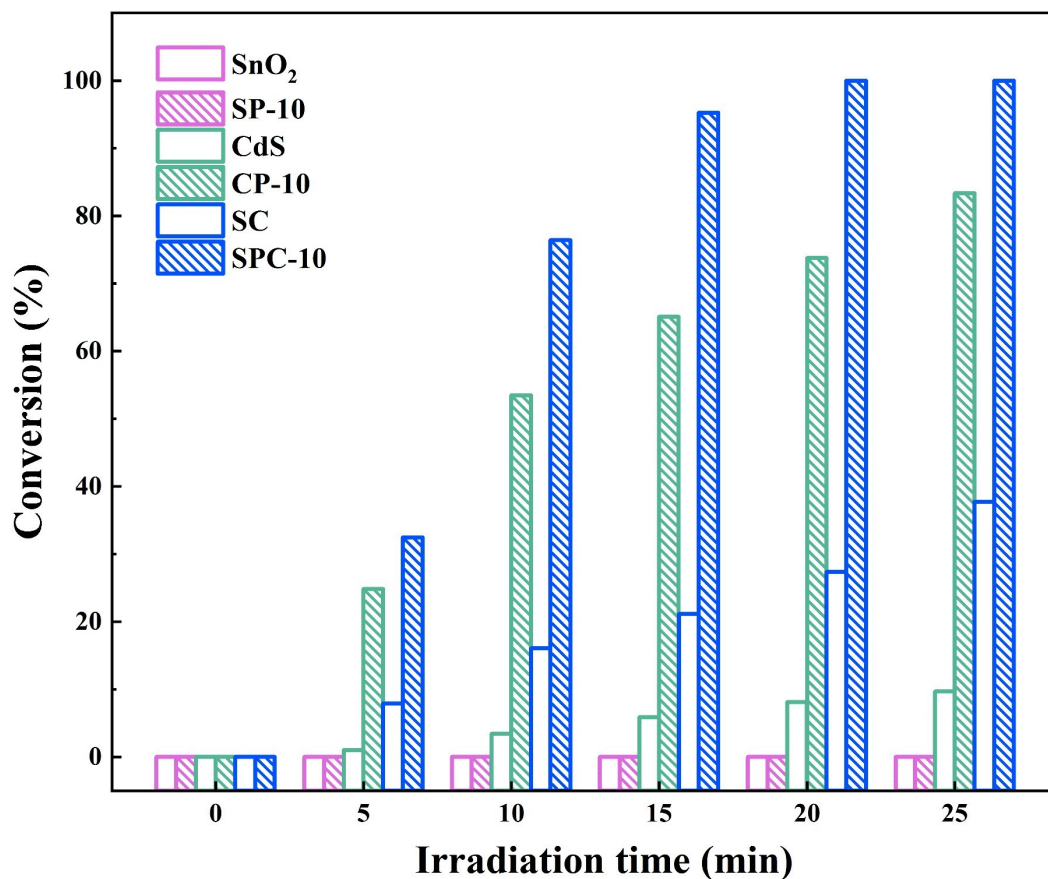


Fig. S15. Photoactivities of SnO₂ NSs, SP-10, CdS, CP-10, SC, and SPC-10 toward 4-NA photoreduction under visible light irradiation ($\lambda > 420$ nm).

Note: Fig. S15 shows that SPC-10 exhibits the optimal photoactivities compared with other counterparts under the same conditions. Photoactivities of the samples toward 4-NA reduction follow the order of SPC-10 > CP-10 > SC > SnO₂ NSs = SP-10 = 0. The enhanced photoactivity of SC relative to SnO₂ NSs suggests that CdS deposition is beneficial for accelerating the interfacial charge transfer owing to the suitable energy level alignment between SnO₂ and CdS. Note that CP-10 and SPC-10 demonstrate considerably enhanced photoactivity relative to CdS and SC, implying ultra-thin PDDA layer plays an indispensable role in boosting the photoreduction performances of CP-10 and SPC-10 for efficiently relaying electrons photoexcited from CdS.

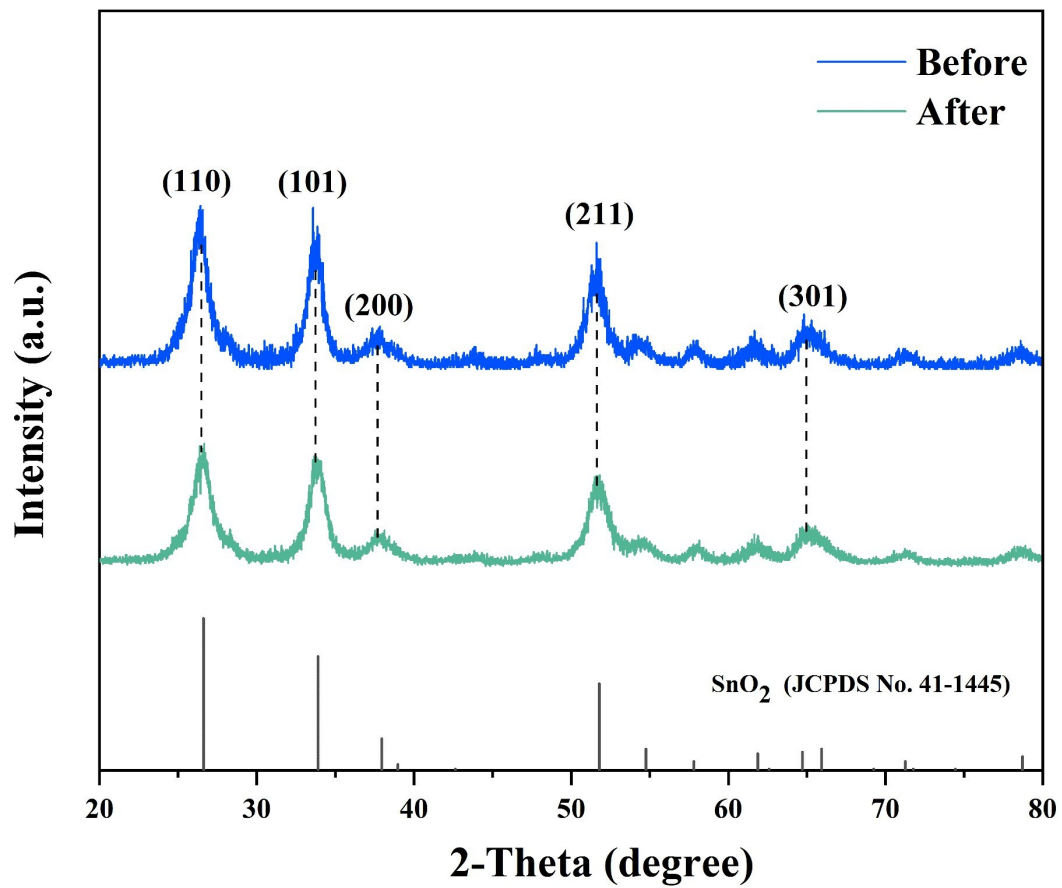


Fig. S16. XRD patterns of SPC-10 before and after cyclic photoreduction reactions.

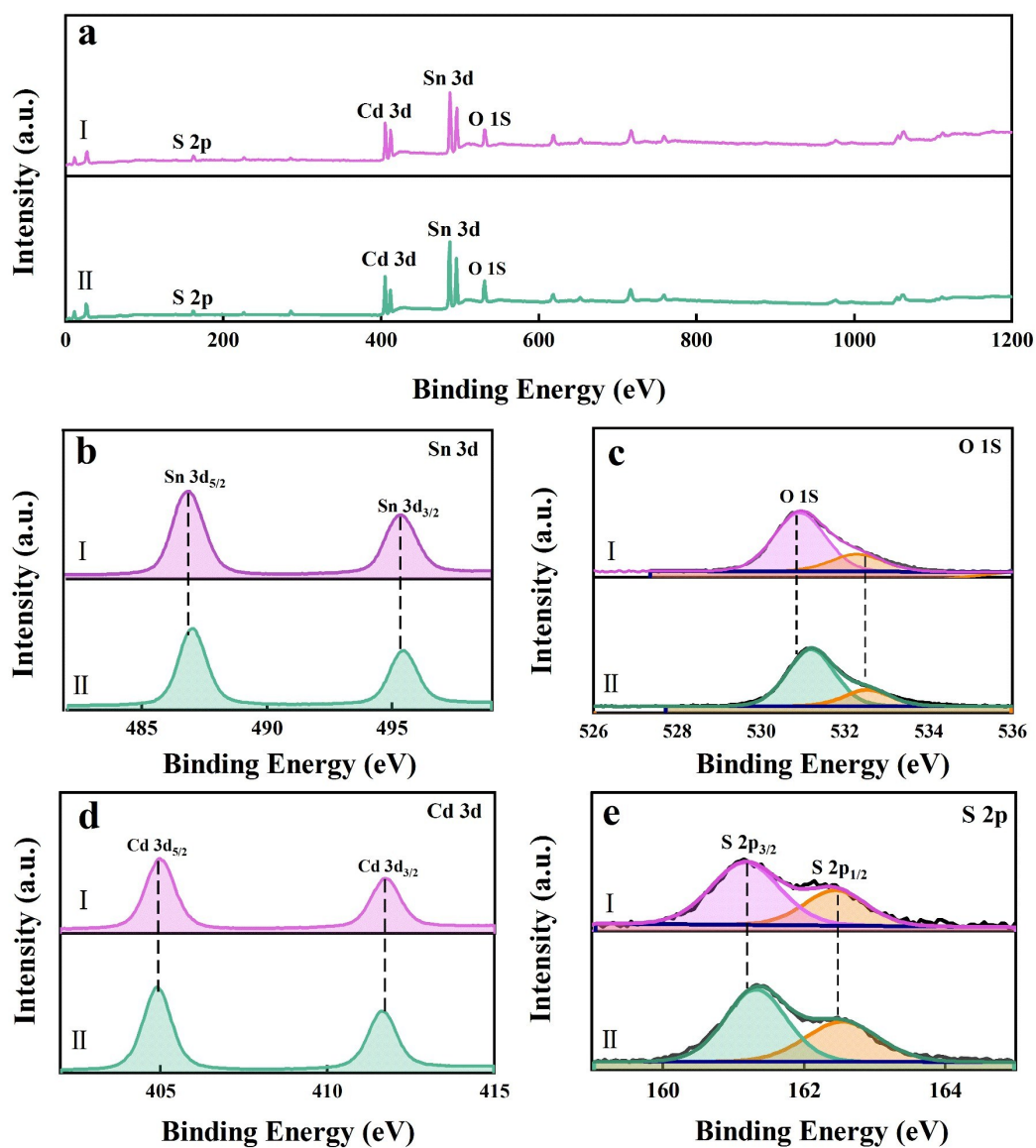


Fig. S17. Survey and high-resolution Sn 3d, O 1s, Cd 3d, and S 2p spectra of SPC-10 (II) before and (I) after cyclic photoreduction reactions.

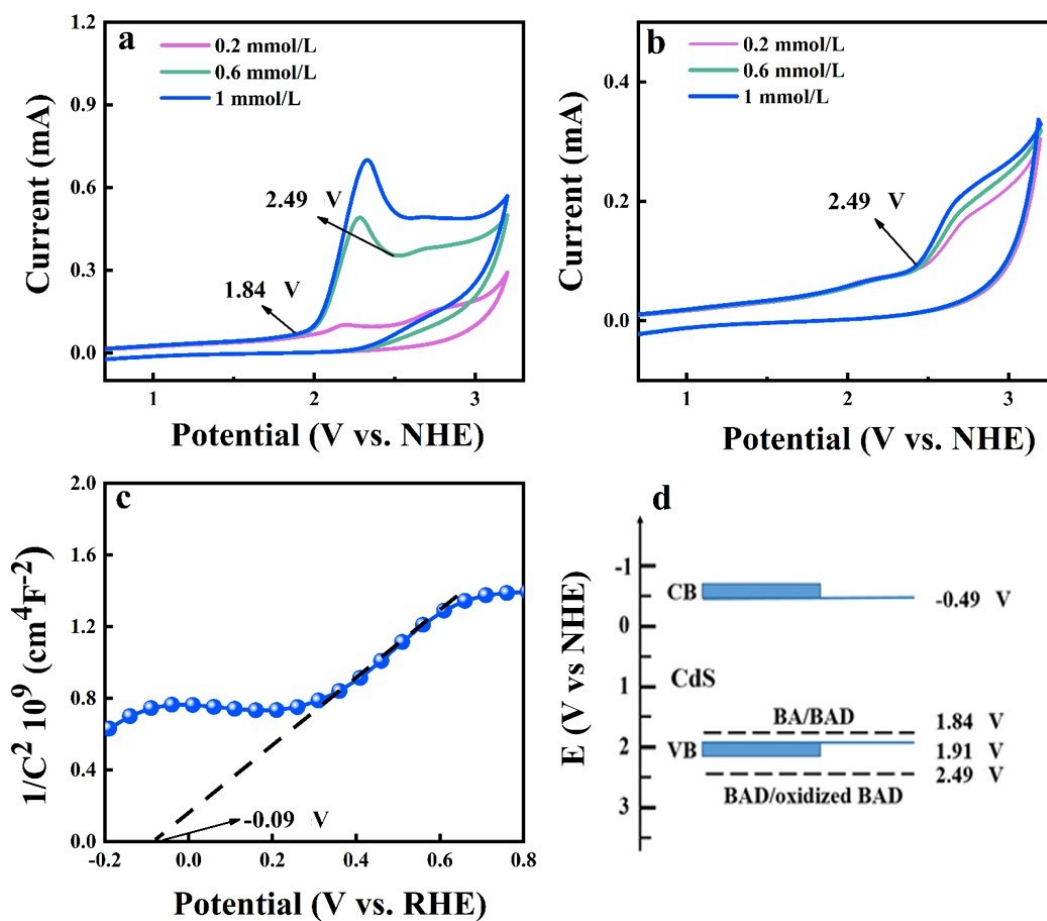


Fig. S18. CV curves of (a) BA and (b) BAD with different concentration (0.2, 0.6, 1 mmol/L), (c) M-S result of CdS, and (d) energy level positions of CdS and redox potentials of BA and BAD.

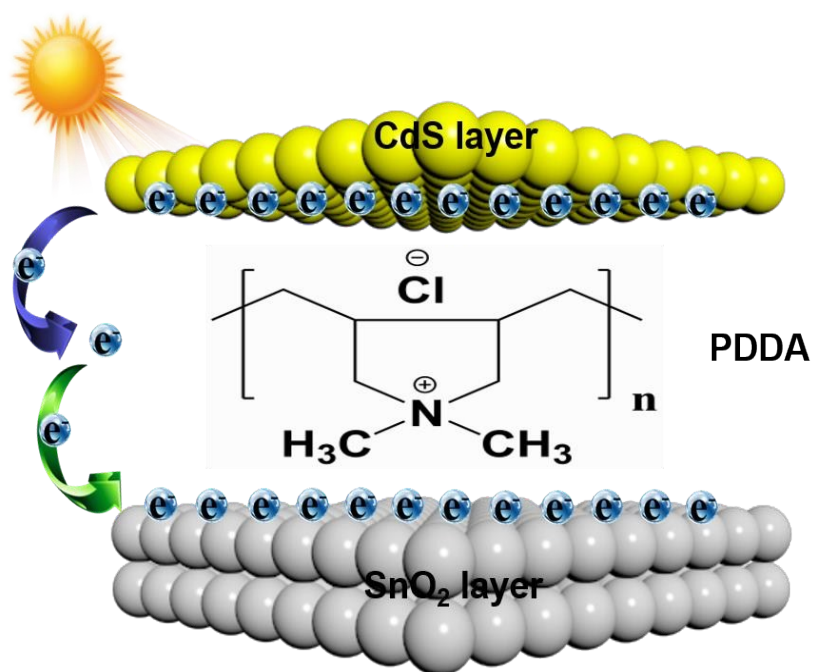


Fig. S19. Schematic illustration of photocatalytic mechanism of SPC and molecular structure of PDDA.

Table S1. Functional groups vs. wavenumber for different samples.

Wavenumber (cm ⁻¹)	Vibration mode	Functional groups or Chemical bonds
3426	$\nu_{\text{O-H}}$	O-H
2850 & 2923	$\nu_{\text{C-H}}$	-CH ₂ -
1635	$\delta_{\text{O-H}}$	O-H
1386	$\delta_{\text{C-H}}$	-CH- & -CH ₃
565	Sn-OH	SnO ₂
667	O-Sn-O	SnO ₂

Table S2. Specific surface area, pore volume and pore size of SnO₂ NSs, SC, and SCP-10.

Samples	S _{BET} (m ² /g) ^a	Total pore volume (cm ³ /g) ^b	Average pore size (nm) ^c
SnO ₂ NSs	132.2750	0.098683	29.8419
SC	106.4320	0.083611	31.4234
SPC-10	93.5180	0.072763	29.9752

^a BET surface area is calculated from the linear part of BET plots. ^b

Single point total pore volume of the pores at P/P₀ = 0.99.

^c Adsorption average pore width (4V/A by BET).

Table S3. Chemical bond species vs. B.E. for different samples.

Element	SnO₂ NSs	SC	SPC-10	Chemical Bond Species
Sn 3d _{3/2}	495.20 eV	489.25 eV	495.35 eV	Sn ⁴⁺
Sn 3d _{5/2}	486.71 eV	486.80 eV	487.70 eV	Sn ⁴⁺
O 1s	530.55 eV	530.82 eV	530.95 eV	O ₂ ⁻
Cd 3d _{3/2}	Not detected	411.65 eV	411.75 eV	Cd ²⁺
Cd 3d _{5/2}	Not detected	404.85 eV	404.95 eV	Cd ²⁺
S 2p _{1/2}	Not detected	162.45 eV	162.55 eV	S ₂ ⁻
S 2p _{3/2}	Not detected	161.15 eV	161.35 eV	S ₂ ⁻

Table S4. Photoactivities of different samples toward selective oxidation of BA to BAD under visible light irradiation ($\lambda > 420$ nm) for 4 h.

Number	Sample	Conversion (%)	Yield (%)	Selective (%)
1	SnO ₂ NSs	0	0	0
2	SC	24	23.8	>99
3	SPC-10	34.5	34.2	>99
4	SP-10	0	0	0
5	CdS	3.4	3.3	>99
6	CP-10	6.1	6.0	>99
7	SrTiO ₃	2.7	2.7	>99
8	SrC	63.9	63.3	>99
9	SrPC-10	77.3	76.7	>99
10	TiO ₂	10.45	10.4	>99
11	TC	77.3	77.1	>99
12	TPC-10	86.5	86.2	>99

Table S5. Photoactivities of different samples toward oxidation of aromatic alcohols under visible light irradiation ($\lambda > 420$ nm) for 4 h.

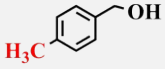
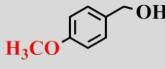
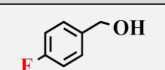
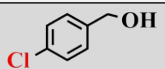
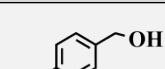
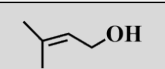
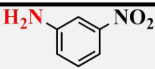
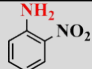
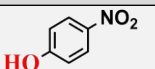
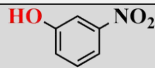
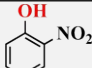
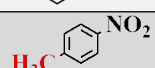
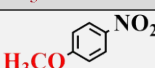
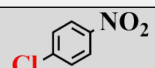
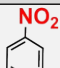
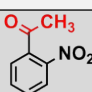
Number	Substrate	Conversion (C), Yield (Y), Selectivity (S)		
		SnO ₂ NSs	SC	SPC-10
a		C 4.7%, Y 4.2%, S 88%	C 34.8%, Y 30.0%, S 86%	C 43.3%, Y 36.6%, S 86%
b		C 13%, Y 11.8%, S 89%	C 39.8%, Y 35.2%, S 88%	C 51.8%, Y 46.6%, S 89%
c		C 1.64%, Y 1.6%, S 98%	C 25.2%, Y 24.5%, S 97%	C 43.2%, Y 41.4%, S 96%
d		C 1.2%, Y 1.1%, S 98%	C 27.1%, Y 22.4%, S 83%	C 37.2%, Y 31.7%, S 85%
e		C 1.3%, Y 1.2%, S 98%	C 20.1%, Y 13.0%, S 62.4%	C 30.2%, Y 22.0%, S 74%
f		C 3.5%, Y 3.2%, S 97%	C 27.9%, Y 16.9%, S 61%	C 34.3%, Y 25%, S 73%

Table S6. Photoactivities of different samples toward 4-NA photoreduction under visible light irradiation ($\lambda > 420$ nm).

Number	Sample	Irradiation time	Conversion (%)
		(min)	
1	SnO ₂ NSs	25	0
2	SC	25	38
3	SPC-10	25	100
4	SP-10	25	0
5	CdS	25	10
6	CP-10	25	83
7	TiO ₂	2	0
8	TC	2	74
9	TPC-10	2	86

Table S7. Photoactivities of different samples toward reduction of a series of nitroaromatic compounds under visible light irradiation ($\lambda > 420$ nm).

Number	Substrate	Conversion (%)		
		SnO ₂ NSs	SC	SPC-10
a		0	24	83
b		0	14	72
c		0	14	87
d		0	30	100
e		0	25	98
f		0	45	100
g		0	70	84
h		0	30	82
i		0	32	58
j		0	31	73

Experimental section

1. Materials

Treatment using titanium (IV) bis (ammonium lactate) dihydroxide (TALH) were purchased from Sigma-Aldrich (China) Co., Ltd. Triethylene glycol (TEG), Urea ($\text{CO}(\text{NH}_2)_2$), $\text{Sr}(\text{OH})_2 \cdot 8\text{H}_2\text{O}$, $\text{NH}_3 \cdot \text{H}_2\text{O}$, Polyvinyl pyrrolidone (PVP) (K30) and acetic acid were obtained from Sinopharm Chemical Reagent Co., Ltd. (Shanghai, China). Tetrabutyl titanate [$\text{Ti}(\text{OBu})_4$] were obtained from Aladdin Industrial Corporation (Shanghai, China). All the reagents were used directly without further purification.

2. Preparation of CdS

CdS by a photo-deposition approach with some modifications. Specifically, $\text{CdCl}_2 \cdot 2.5\text{H}_2\text{O}$ and S_8 were dispersed in 200 mL of methanol to form a stable suspension and bubbled with N_2 for 30 min in the dark and then irradiated with simulated solar light by using a 300 W Xe arc lamp (PLS-SXE300D, Beijing Perfect Light co. LTD, China). The samples were rinsed with DI H_2O and absolute ethanol and then dried in vacuum at 60 °C for 4 h.

3. Preparation of SP-10 and CP-10

SnO_2 or CdS was added into the PDDA aqueous solution (20 mL) with concentration of 10 mg mL^{-1} , and vigorously stirred for 30 min. After that, The samples was sufficiently rinsed with DI H_2O and dried in vacuum at 60 °C for 4 h. The obtained samples were denoted as SnO_2 NSs@PDDA-10 (SP-10) or CdS@PDDA-10 (CP-10).

4. Preparation of SrTiO_3

SrTiO_3 nanocubes were synthesized by using a modified method.¹ Namely, 32 mmol $\text{Sr}(\text{OH})_2 \cdot 8\text{H}_2\text{O}$, 32 mmol $\text{Ti}(\text{OBu})_4$, 16 mL $\text{NH}_3 \cdot \text{H}_2\text{O}$ and 1.48 g PVP were together added into a flask with 80 mL TEG. After that, the mixture was heated at 160 °C for 2 h with strong stirring. Following that, 20 mL acetic acid was added to remove the by-product SrCO_3 when the obtained light yellow sol was cooled to room temperature. The further reaction for 30 min, the end-product (white powder) was received after resulting composite being thoroughly washed with water and ethanol, respectively, and dried at 60 °C for 6 h in a vacuum oven.

5. Preparation of TiO_2

TiO_2 NPs were synthesized by homogeneous hydrolysis combined with a hydrothermal treatment using titanium (IV) bis (ammonium lactate) dihydroxide (TALH) as the precursor.² specifically, 13.8 g of urea was added to a diluted TALH aqueous solution (1.52 mL TALH, 50 mL DI H_2O), which was vigorously

stirred for 1 h at ambient conditions. The mixture was then put in an oil bath at 95 °C for 24 h under magnetic stirring and refluxing. After cooling to room temperature, a gel-like precipitate was obtained after centrifugation and washed twice with DI H₂O. The washed gel was subsequently dispersed in DI H₂O and sealed in a Teflon-lined autoclave (100 mL) at 150 °C for 24 h to improve the crystallinity of the TiO₂ NPs.

6. Preparation of SrC and TC

CdS layer was coated on the SrTiO₃ or TiO₂ surface by a photodeposition approach with some modifications. In a typical procedure, 80 mg of CdCl₂·2.5H₂O and 20 mg of S₈ were dispersed in 200 mL of methanol to form a stable suspension and bubbled with N₂ for 30 min in the dark. The 200 mg of TiO₂ or SrTiO₃ was immersed in the above suspension and irradiated with simulated solar light for 7 h by using a 300 W Xe arc lamp (PLS-SXE300D, Beijing Perfect Light co. LTD, China). The samples were rinsed with DI water and absolute ethanol and then dried in vacuum at 60 °C for 4 h. The obtained samples were denoted as SrTiO₃@CdS (SrC) and TiO₂@CdS (TC).

7. Preparation of SrPC-10 and TPC-10

200 mg of SrTiO₃ or TiO₂ was added into the aqueous PDDA solution (10 mg/mL, 20 mL) and vigorously stirred for 30 min. PDDA-modified SrTiO₃ or TiO₂ (SrTiO₃@PDDA or TiO₂@PDDA) were sufficiently rinsed with DI H₂O and dried in vacuum at 60 °C for 4 h. Subsequently, CdS layer was coated on the SrTiO₃@PDDA or TiO₂@PDDA surface by a photodeposition approach as mentioned above. The obtained samples were denoted as SrTiO₃@PDDA-10@CdS (SrPC-10) and TiO₂@PDDA-10@CdS (TPC-10).

References

1. X.-L. Yin, L.-L. Li, D.-C. Li, D.-H. Wei, C.-C. Hu and J.-M. Dou, *J. Colloid Interface Sci.*, 2019, **536**, 694-700.
2. S. Yuan, J. Mu, R. Mao, Y. Li, Q. Zhang and H. Wang, *ACS Appl. Mater. Interfaces*, 2014, **6**, 5719-5725.